7-1999

Interannual Variations in Snowmelt Onset and Links to 500 hPa Atmospheric Anomalies over the Arctic

Sheldon D. Drobot
National Center for Atmospheric Research, drobot@ucar.edu

Mark R. Anderson
University of Nebraska-Lincoln, manderson4@unl.edu

Interactions Between the Cryosphere, Climate and Greenhouse Gases (Proceedings of IUGG 99 Symposium HS2, Birmingham, July 1999). IAHS Publ. no. 256, 1999.

Interannual variations in snowmelt onset and links to 500 hPa atmospheric anomalies over the Arctic

SHELDON DROBOT & MARK ANDERSON

Department of Geosciences, University of Nebraska, Lincoln, Nebraska 68588, USA
e-mail: sdrobot@unlgrad1.unl.edu

Abstract Interannual variations in the melt onset of snow provide a mechanism to observe climatic fluctuations. Timing of initial ablation is associated with certain poorly defined overlying atmospheric conditions. This paper investigates the spatial and temporal patterns in melt onset dates and associated 500 hPa height anomalies over the Arctic region from 1982 to 1992. Melt onset dates are derived from Scanning Multichannel Microwave Radiometer (SMMR) and Special Sensor Microwave Imager (SSM/I) data, while 500 hPa height anomalies are computed from the National Centers for Environmental Protection (NCEP) reanalysis models. Results indicate significant interannual variations in the spatial pattern and timing of melt onset. With the assistance of principal component analysis (PCA) links between the melt onset dates and the 500 hPa height anomaly field are highlighted.

INTRODUCTION

Snow cover on sea ice is an integral component of the global climate system owing to its influence on sea ice growth and ablation (Brown & Cote, 1992), energy and mass transfer (Maykut, 1986), and ocean thermohaline circulation (Yang & Neelin, 1993). The significance of snow cover is particularly emphasized during the onset of melt since energy absorption over a wet snowpack can be an order of magnitude greater than energy absorption over a dry snowpack (Grenfell & Perovich, 1984). Climatological concern centres on the ramifications that interannual variations in the spatial and temporal pattern of snowmelt onset may pose for the global climate.

Originally, the spatial pattern of snowmelt onset across the Arctic was thought to occur latitudinally in response to increased solar radiation during the spring transition (Marshunova & Chernigoviskiy, 1966). However, empirical observations from Soviet ice stations (Yanes, 1966) and aircraft reconnaissance (Kuznetsov & Timerev, 1973) illustrate the melt onset pattern is much more complex than initially thought. It is still believed the spatial pattern of melt onset responds to atmospheric conditions such as advection of sensible heat, but the exact physical linkages remain poorly defined.

The advent of microwave radiometry has greatly increased our understanding of the spatial pattern and timing of snowmelt onset. For instance, Abdalati & Steffen (1995) and Mote & Anderson (1995) used Scanning Multichannel Microwave Radiometer (SMMR) and Special Sensor Microwave Imager (SSM/I) satellite data to illustrate large interannual variability in the timing of melt onset as well as the spatial melt pattern over the Greenland ice sheet. More recently, Anderson (1997) reported

melt onset variations up to 11 days over first-year ice from 1989 to 1991. Melt onset over multiyear ice (MYI) showed an even greater variation of 36 days. Along similar lines, Smith (1998) reported the summer melt season of sea ice has increased 8% from 1979 to 1996.

Research illustrating the coupling of the atmosphere to spatial and temporal variations in snowmelt onset is virtually non-existent. Of the published works considering the atmosphere, most focus on atmosphere–sea ice interactions. For instance, Serreze *et al.* (1995) noted the record minimum in sea-ice extent in 1990 was associated with anomalously low mean sea level pressures over the Arctic region. Using case studies in the Beaufort Sea and Canadian Basin, Maslanik *et al.* (1995) documented situations where the passage of low pressure systems immediately altered the ice conditions. Maslanik *et al.* (1996) further proposed decreased sea-ice extents noticed in the 1990s were directly linked to an increased incidence of low pressure systems over the Arctic. However, these studies did not examine snow during the melt onset period.

The primary objective of this paper is to illustrate interannual variations in snowmelt onset and the associated 500 hPa height anomalies over the Arctic. Specifically, this paper will:

(a) analyse interannual variability in snowmelt onset from 1982 to 1992 amongst 13 case study sites distributed across the Arctic, and
(b) highlight similarities between variations in melt onset and 500 hPa height anomalies with the aid of principal component analysis (PCA).

DATA

Melt onset dates from microwave radiometry

Microwave data used in this study were acquired from the SMMR and the SSM/I platforms. SMMR data were analysed for 1982–1986 and SSM/I data were analysed from 1988 to 1992. The melt season was defined to be between 1 April and 31 July. Melt onset dates were not calculated for 1987 since neither sensor was operational during the entire melt season and no attempt was made to standardize the passive microwave brightness temperature data. Further details on SMMR can be found in Gloersen & Hardis (1978), while information on the SSM/I sensor is available from Hollinger *et al.* (1990).

Exploiting the melt onset algorithm developed by Anderson (1997), this paper examined melt onset dates of snow over 13 case study sites distributed across the Arctic (Fig. 1 and Table 1). The melt onset algorithm uses the difference between the 19 GHz (18 GHz SMMR) and 37 GHz horizontally polarized channel (HG algorithm) and is given by:

$$\mathrm{HR} = T_B(19\mathrm{H}) - T_B(37\mathrm{H})$$

The horizontal channels reflect a strong dependence on snow conditions during melt. Rapid changes in snow conditions are observed in the brightness temperatures. During melt conditions, the brightness temperatures first increase due to the inclusion of liquid

water within the snowpack, then decrease because freeze/thaw cycles enlarge the snow grain size (i.e. Mätzler, 1987; Onstott *et al.*, 1987). Complete details of the algorithm are available in Anderson (1997).

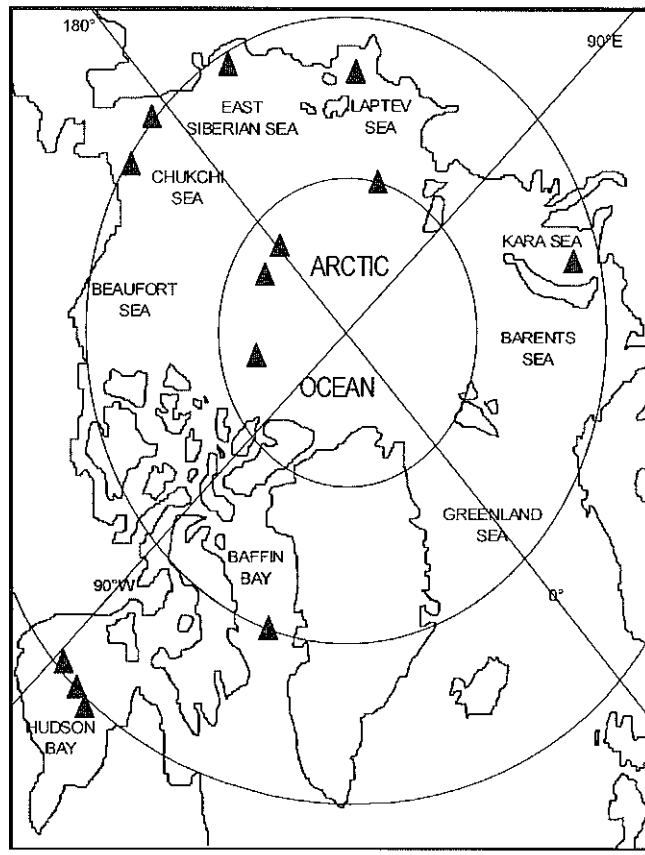

Fig. 1 Study region with case study sites represented by triangles.

Table 1 Location sites.

Pt	Location	Latitude	Longitude
1	Laptev Sea (FY1)	72°N	135°E
2	East Siberian Sea (FY1)	71N	165°E
3	Chukchi Sea (FY1)	69°N	176°W
4	Chukchi Sea (FY1)	70°N	167°W
5	Laptev Sea (MYI)	80°N	120°E
6	Barents Sea (FY1)	72°N	62°E
7	Arctic Ocean (MYI)	83°N	180°E
8	Arctic Ocean (MYI)	83°N	177°W
9	Arctic Ocean (MYI)	83°N	136°W
10	Baffin Bay (FY1)	70°N	60°W
11	Hudson Bay (FY1)	60.5°N	88°W
12	Hudson Bay (FY1)	59°N	85°W
13	Hudson Bay (FY1)	57°N	82.5°W

500 hPa height anomalies

The 500 hPa height anomalies were computed from the National Centers for Environmental Protection (NCEP) reanalysis data CDs. Monthly 500 hPa data fields were extracted for April and May from 1982 to 1992 to calculate mean height fields for each month. The anomaly fields were calculated on a pixel by pixel basis as the deviation from each month's average height field over the entire time series. Specific pixels were extracted to match the geographic coordinates of the snowmelt onset date calculations. In this paper, height anomalies for the months of April and May are used.

ANALYSIS METHODS

Descriptive statistics were employed to analyse the temporal pattern in melt onset over the 13 case studies. A principal component analysis on 500 hPa height anomalies was employed to describe the inter-relationship between melt onset and height anomaly data. PCA analysis is useful because it can reveal relationships in the data that were not previously suspected and thereby allows for interpretation that would not normally result. In this work two PCs are used to illustrate the linkages between melt onset and spatial variation in 500 hPa height anomalies. The first principal component (PC1) is the linear combination of data variables that maximizes variance. The second principal component (PC2) is the linear combination of data variables that maximizes variance subject to the constraint that the covariance between PC1 and PC2 is zero. Scatter plots of PC1 *vs* PC2 were also used to aid in the interpretation of the results.

RESULTS

Interannual variability in melt onset of snow

Using the HR algorithm, results indicate large interannual variations in melt onset dates between sites. For instance, melt onset dates vary by more than two months over several first-year sites (Table 2). Conversely, many of the multiyear ice locations exhibit noticeably smaller interannual melt onset variations. In general, the southernmost locations, such as points in Hudson Bay, usually experience melt onset in the early part of April, while the more northern locations in the Arctic Ocean typically undergo melt onset from mid to late June.

The results also indicate strong annual variations among individual locations. It should be noted that the HR algorithm detects the initial melting of the snowpack instead of the initialization of continuous melting. Therefore, it is likely that melt/freeze cycles are taking place after the initial onset of melt. Nevertheless, the onset of any melting will be accompanied by a change in surface albedo with corresponding changes in energy transfer across the atmosphere–sea ice–ocean interface. Anderson (1997) has also shown that when melting occurs the sea ice concentrations produced by the NASA Team algorithm are not always accurate.

To illustrate the spatial variability in the melt onset dates, two sites, a first-year and multiyear ice location will be discussed in more detail, noting that other sites

Table 2 Melt onset dates (Julian days) for locations listed in Table 1.

Location	1982	1983	1984	1985	1986	1988	1989	1990	1991	1992	Average	Std
1	156	105	164	94	159	171	134	123	129	141	138	26
2	142	169	138	118	161	165	99	92	91	157	133	31
3	148	165	164	156	165	161	141	101	142	143	149	19
4	96	91	140	138	107	120	96	115	111	94	111	18
5	170	127	180	108	141	176	169	149	147	125	149	24
6	118	151	104	152	101	135	104	103	98	126	119	21
7	186	187	160	174	179	163	174	138	158	172	169	15
8	186	179	160	174	163	163	174	138	185	172	169	14
9	176	179	170	168	159	182	173	157	186	172	172	9
10	92	99	102	92	103	157	108	115	122	113	110	19
11	92	91	94	94	95	123	104	93	97	92	98	10
12	98	113	124	96	95	123	117	92	111	128	110	13
13	92	93	124	104	111	100	134	93	111	99	106	14
Average	135	135	140	128	134	149	133	116	130	133		
Std	38	38	29	33	32	26	31	23	32	29		

have very similar results. The first-year ice location chosen is in the Barents Sea (Point 6). The earliest melt onset occurred on 8 April 1991 (Julian day 98) while the latest detected melt was on 6 June 1981 (Julian day 157). The range of melt onset dates was 59 days, with the average onset date being 2 May (Julian day 122). In comparison the site in the Arctic Ocean (Point 8) detected melt for the first time on 18 May 1990 (Julian day 138). The latest detected melt occurred on 5 July 1982 (Julian day 186). The range in melt dates for this site was only 48 days. As expected, the southern locations have the greater range in melt dates. The average melt onset date for the Arctic Ocean location was also 47 days later than the Barents Sea location. In general, the standard deviations for first-year ice locations are commonly larger than for multiyear ice locations, again illustrating the larger variations in melt onset for the more southern locations along the marginal ice zone.

Principal component analysis of the 500 hPa height anomalies

The first principal component, PC1 (explains 44% of total variation), is roughly a measure of the typical height anomaly across the Arctic region excluding Hudson Bay (Table 3). Specifically, PC1 suggests height anomalies tend to vary in unison from 90°E to 90°W. When the anomaly is positive over the Arctic Ocean it is typically also positive over the Laptev, Chukchi, and East Siberian Sea regions as well.

The second principal component, PC2 (explains 27% of total variation), represents diversity in the Hudson Bay and Barents Sea regions not seen in PC1. It also roughly indicates a high PC2 score is associated with positive anomalies in the Hudson Bay and Barents region, but negative anomalies in the Laptev to Chukchi Sea region. In light of this, PC2 may be considered to account for regional variations, and is likely associated with the Rossby wave pattern. In a 4-wave situation, high heights over the Hudson Bay region should be mirrored with high heights over the Barents Sea, with corresponding low heights over the Chukchi to Laptev Sea region.

Table 3 Correlation of PCs with location.

Location	PC1	PC2
Laptev Sea	0.77	−0.19
East Siberian Sea	0.75	−0.35
Chukchi Sea	0.74	−0.45
Chukchi Sea	0.73	−0.50
Laptev Sea (MYI)	0.83	0.32
Barents Sea	0.25	0.71
Arctic Ocean (MYI)	0.99	0.05
Arctic Ocean (MYI)	0.99	0.05
Arctic Ocean (MYI)	0.93	0.00
Baffin Bay	0.61	−0.41
Hudson Bay	0.06	0.82
Hudson Bay	0.11	0.83
Hudson Bay	0.18	0.86

Relationship between melt onset of snow and 500 hPa height anomalies

A relationship between the interannual variations in the average melt onset date of all sites within a year and the 500 hPa height anomalies is apparent when comparing PC1 and PC2 scores. Early melt dates across the Arctic region (Table 2) are associated with high PC2 scores and low PC1 scores (Fig. 2). For instance, the two latest average melt dates are day 149 (1988) and day 140 (1984), which distinctly appear in the upper left quadrant of the scatter plot. The earliest average melt date is day 116 (1990), which is associated with the lower left quadrant of the scatter plot. Generally, it appears low heights over the Arctic region in April are associated with early snowmelt dates. Physically, lower pressures and warm air advection associated with lower heights could trigger an earlier melt.

CONCLUSIONS

A study was launched to detect the onset of snowmelt for selected locations within the Arctic sea ice basin and highlight the association to 500 hPa height anomalies. Results from this investigation show that melt onset dates can vary by more than two months both across the Arctic and interannually within each location. Principal component analysis proved to be useful in highlighting variability within the 500 hPa height anomaly fields and for highlighting similarities to the onset of snowmelt. PC1

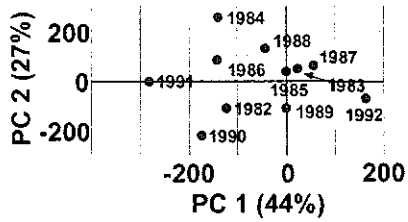

Fig. 2 Scatter plot of data on PC1 *vs* PC2 of the 500 hPa height anomalies.

represented a general picture of the Arctic height anomalies, while PC2 underlined some regional differences. High PC1 and low PC2 scores are associated with earlier than normal melt onset dates.

Future research will broaden the data set to include the entire Arctic region so relationships can be more clearly defined. Plans to analyse the spatial and temporal variations in both melt onset date and 500 hPa height anomalies should reveal previously unknown relationships. In turn these can be used to further our understanding of atmosphere–sea ice–ocean interactions operating within the Arctic, and help provide answers to climate change questions.

REFERENCES

Abdalati, W. & Steffen, K. (1995) Passive microwave-derived snowmelt regions on the Greenland ice sheet. *Geophys. Res. Lett.* **22**, 787–790.

Anderson, M. R. (1997) Determination of a melt onset date for Arctic sea ice regions using passive microwave data. *Ann. Glaciol.* **25**, 382–387.

Brown, R. D. & Cote, P. (1992) Interannual variability of landfast ice thickness in the Canadian High Arctic, 1950–89. *Arctic* **45**, 273–284.

Gloersen, P. & Hardis, L. (1978) The scanning multichannel microwave radiometer (SMMR) experiment. In: *The Nimbus 7 User's Guide* (ed. by C. Madrid), 213–243. NASA, Washington, DC.

Grenfell, T. G. & Perovich, D. K. (1984) Spectral albedo of sea ice and incident solar irradiance in the Southern Beaufort Sea. *J. Geophys Res.* **89**, 3573–3580.

Hollinger, J. P., Pierce, J. L. & Poe, G. A. (1990) SSM/I instrument evaluation. *IEEE Trans. on Geosci. Remote Sensing* **28**, 781–790.

Kuznetsov, I. M. & Timerev, R. A. (1973) The dependence of ice albedo on the ice cover state as determined by airborne observations. *Problems of the Arctic and Antarctic* (ed. by A. F. Treshnikov) **40**, 67–74.

Marshunova, M. S. & Chernigovskiy, N. T. (1966) Numerical characteristics of radiation regime in the Soviet Arctic. In: *Symposium on Arctic Heat Budget and Atmospheric Circulation* (ed. by J. O. Fetcher) (31 January–4 February 1966, Lake Arrowhead, California). Rand Memorandum RM-5233-NSF.

Maslanik, J. A., Fowler, C., Heinrichs, J., Barry, R. G. & Emery, W. J. (1995) Remotely-sensed and simulated variability of Arctic sea-ice concentrations in response to atmospheric synoptic systems. *Int. J. Remote Sensing* **16**, 3325–3342.

Maslanik, J. A., Serreze, M. C. & Barry R. G. (1996) Recent decreases in Arctic summer ice cover and linkages to atmospheric circulation anomalies. *Geophys. Res. Lett.* **23**,1677–1680.

Mätzler, C. (1987) Applications of the interaction of microwaves with the natural snow cover. *Remote Sensing Rev.* **2**(2), 259–387.

Maykut, G. A. (1986) The surface heat and mass balance. Chapter 5 in: *Geophysics of Sea Ice* (ed. by N. Untersteiner), 395–463. Martinus Nijhoff, Dordrecht.

Mote, T. L. & Anderson, M. R. (1995) Variations in snowpack melt on the Greenland ice sheet based on passive-microwave measurements. *J. Glaciol.* **41**, 51–60.

Onstott, R. G., Greenfell, T. C., Matzler, C., Luther, C. A. & Svendsen, E. A. (1987) Evolution of microwave sea ice signatures during early summer and midsummer in the marginal ice zone. *J. Geophys Res.* **92**, 6825–6835.

Serreze, M. C., Maslanik, J. A., Key, J. R., Kokaly, R. F. & Robinson, D. A. (1995) Diagnosis of the record minimum in Arctic sea-ice during 1990 and associated snow cover extremes. *Geophys. Res. Lett.* **22**, 2183–2186.

Smith, D. M. (1998) Recent increase in the length of the melt season of perennial Arctic sea ice. *Geophys. Res Lett.* **25**, 655–658.

Yanes, A. V. (1966) Melting snow and ice in the central Arctic. *Problems of the Arctic and Antarctic* (ed. by N. A. Osterso) **11**, 1–13.

Yang, J. & Neelin, D. J. (1993) Sea-ice interaction with the thermohaline circulation. *Geophys. Res. Lett.* **20**, 217–220.